

Original research

# *Helicobacter pylori* promotes colorectal carcinogenesis by deregulating intestinal immunity and inducing a mucus-degrading microbiota signature

Anna Ralser,<sup>1</sup> Alisa Dietl,<sup>1</sup> Sebastian Jarosch,<sup>1,2</sup> Veronika Engelsberger,<sup>1</sup> Andreas Wanisch,<sup>1</sup> Klaus Peter Janssen ,<sup>3</sup> Moritz Middelhoff,<sup>4</sup> Michael Vieth,<sup>5</sup> Michael Quante ,<sup>4,6</sup> Dirk Haller ,<sup>7,8</sup> Dirk H Busch,<sup>1,9</sup> Li Deng,<sup>10,11</sup> Raquel Mejías-Luque ,<sup>1,9</sup> Markus Gerhard <sup>1,9</sup>

► Additional supplemental material is published online only. To view, please visit the journal online (<http://dx.doi.org/10.1136/gutjnl-2022-328075>).

For numbered affiliations see end of article.

## Correspondence to

Professor Markus Gerhard, Institute for Medical Microbiology, Immunology and Hygiene, School of Medicine, Technical University of Munich, München 80333, Germany; [markus.gerhard@tum.de](mailto:markus.gerhard@tum.de)

RM-L and MG contributed equally.

Received 15 June 2022  
Accepted 19 March 2023  
Published Online First  
4 April 2023



© Author(s) (or their employer(s)) 2023. No commercial re-use. See rights and permissions. Published by BMJ.

**To cite:** Ralser A, Dietl A, Jarosch S, et al. *Gut* 2023;**72**:1258–1270.

## ABSTRACT

**Objective** *Helicobacter pylori* infection is the most prevalent bacterial infection worldwide. Besides being the most important risk factor for gastric cancer development, epidemiological data show that infected individuals harbour a nearly twofold increased risk to develop colorectal cancer (CRC). However, a direct causal and functional connection between *H. pylori* infection and colon cancer is lacking.

**Design** We infected two *Apc*-mutant mouse models and C57BL/6 mice with *H. pylori* and conducted a comprehensive analysis of *H. pylori*-induced changes in intestinal immune responses and epithelial signatures via flow cytometry, chip cytometry, immunohistochemistry and single cell RNA sequencing. Microbial signatures were characterised and evaluated in germ-free mice and via stool transfer experiments.

**Results** *H. pylori* infection accelerated tumour development in *Apc*-mutant mice. We identified a unique *H. pylori*-driven immune alteration signature characterised by a reduction in regulatory T cells and pro-inflammatory T cells. Furthermore, in the intestinal and colonic epithelium, *H. pylori* induced pro-carcinogenic STAT3 signalling and a loss of goblet cells, changes that have been shown to contribute—in combination with pro-inflammatory and mucus degrading microbial signatures—to tumour development. Similar immune and epithelial alterations were found in human colon biopsies from *H. pylori*-infected patients. Housing of *Apc*-mutant mice under germ-free conditions ameliorated, and early antibiotic eradication of *H. pylori* infection normalised the tumour incidence to the level of uninfected controls.

**Conclusions** Our studies provide evidence that *H. pylori* infection is a strong causal promoter of colorectal carcinogenesis. Therefore, implementation of *H. pylori* status into preventive measures of CRC should be considered.

## INTRODUCTION

*Helicobacter pylori* infection affects more than half of the world's population and it is a main risk factor for gastric cancer. *H. pylori* induces a

## WHAT IS ALREADY KNOWN ON THIS TOPIC

- ⇒ *Helicobacter pylori* infection is the most prevalent bacterial infection worldwide and is the most important risk factor for gastric cancer development.
- ⇒ Infected individuals harbour a nearly twofold increased risk to develop colorectal cancer (CRC).

## WHAT THIS STUDY ADDS

- ⇒ *H. pylori* infection accelerates intestinal tumour development in *Apc*-mutant mice.
- ⇒ *H. pylori* infection induces a pro-inflammatory and pro-carcinogenic environment in murine and human colon.
- ⇒ The observed phenotype was normalised upon eradication therapy and is strongly dependent on microbiota.

## HOW THIS STUDY MIGHT AFFECT RESEARCH, PRACTICE OR POLICY

- ⇒ We provide evidence that *H. pylori* infection is a strong causal promoter of colorectal carcinogenesis and should be included into an adapted risk score for CRC.
- ⇒ Eradication of *H. pylori* infection might be an effective measure to reduce this risk.

number of alterations in the gastric mucosa that together result in neoplastic transformation of the epithelium. Thus, *H. pylori* infection first triggers a complex plethora of immune cascades, directed towards *H. pylori* and orchestrated by the bacterium itself, which originate from priming at the Peyer's patches and the mesenteric lymph nodes of the small intestine.<sup>1,2</sup> The major pro-inflammatory response towards *H. pylori* consists of a mixed T helper (Th)1 and Th17 response,<sup>1</sup> and is to a large extent related to the presence and activity of a type 4 secretion system,<sup>3</sup> which mediates translocation of the oncogenic and highly immunogenic protein CagA into gastric epithelial cells.<sup>4</sup> This leads to chronic inflammation and results in the activation

of pro-inflammatory signalling pathways such as activating nuclear factor- $\kappa$ B (NF- $\kappa$ B) and signal transducer and activator of transcription 3 (STAT3) signalling, which are major drivers of *H. pylori*-induced gastric carcinogenesis.<sup>5</sup> However, *H. pylori* has evolved counter mechanisms in order to establish and maintain chronic infection, for example, by reprogramming dendritic cells (DCs) to induce regulatory T cells (Treg),<sup>6,7</sup> which counterbalance the local pro-inflammatory response in the stomach,<sup>8</sup> and are involved in protection from allergic asthma.<sup>9</sup> Interestingly, this tolerogenic reprogramming of DCs is partially mediated by CagA, via activation of STAT3.<sup>7</sup> Finally, alterations in gastric microbiota are observed on infection, which seem to contribute to the deleterious events leading to gastric cancer following *H. pylori* infection.<sup>10</sup> This idea is supported by studies using animal models as the insulin-gastrin (INS-GAS) mice, which showed more severe gastric pathology and early development of neoplasia when colonised with *H. pylori* and carrying normal commensal microbiota compared with germ-free INS-GAS mice infected with the bacterium.<sup>11</sup>

Although *H. pylori* infection is limited to the stomach, accumulating epidemiological data indicate an association between *H. pylori* infection and different extragastric diseases.<sup>12</sup> Among those, a higher risk of colorectal cancer (CRC) has been reported to be associated with *H. pylori* infection status.<sup>13</sup> However, the mechanisms that could explain this increased risk have not been elucidated.

In our study, we identify *H. pylori*-specific alterations in gut homeostasis that contribute to colorectal carcinogenesis in mouse models of CRC as well as in human samples, and are reversible on *H. pylori* eradication. These findings provide

a basis for assessing *H. pylori* status for gastric, and for colon cancer prevention programmes.

## RESULTS

### *H. pylori* promotes intestinal carcinogenesis in adenomatous polyposis coli mouse models

To determine whether *H. pylori* infection promotes the development of tumours in the lower gastrointestinal (GI) tract, we infected *Apc*<sup>+/*min*</sup> and *Apc*<sup>+/*1638N*</sup> mice for different time periods (online supplemental figure 1A,B). Unexpectedly, *Apc*<sup>+/*min*</sup> mice were highly susceptible to the infection, with only 60% of the mice surviving after 12 weeks of *H. pylori* infection (figure 1A). An increased tumour burden in the small intestine and colon was observed in infected *Apc*<sup>+/*min*</sup> mice compared with uninfected controls (figure 1B,C). Similar results were observed in *Apc*<sup>+/*1638N*</sup> mice, which developed twice as many tumours after infection, and showed larger tumours in the small intestine (online supplemental figure 1C). Notably, in *Apc*<sup>+/*1638N*</sup> mice, colonic tumours were exclusively detected in *H. pylori*-infected mice (online supplemental figure 1C). These observations demonstrate that *H. pylori* infection promotes the development of intestinal and colonic tumours in tumour-prone mice, while exclusively infecting the stomachs of these mice (online supplemental figure 1B).

### *H. pylori* infection induces a pro-inflammatory response in the intestine

Manipulation of host's T-cell immune responses characterises *H. pylori* infection and is one of the main mechanisms

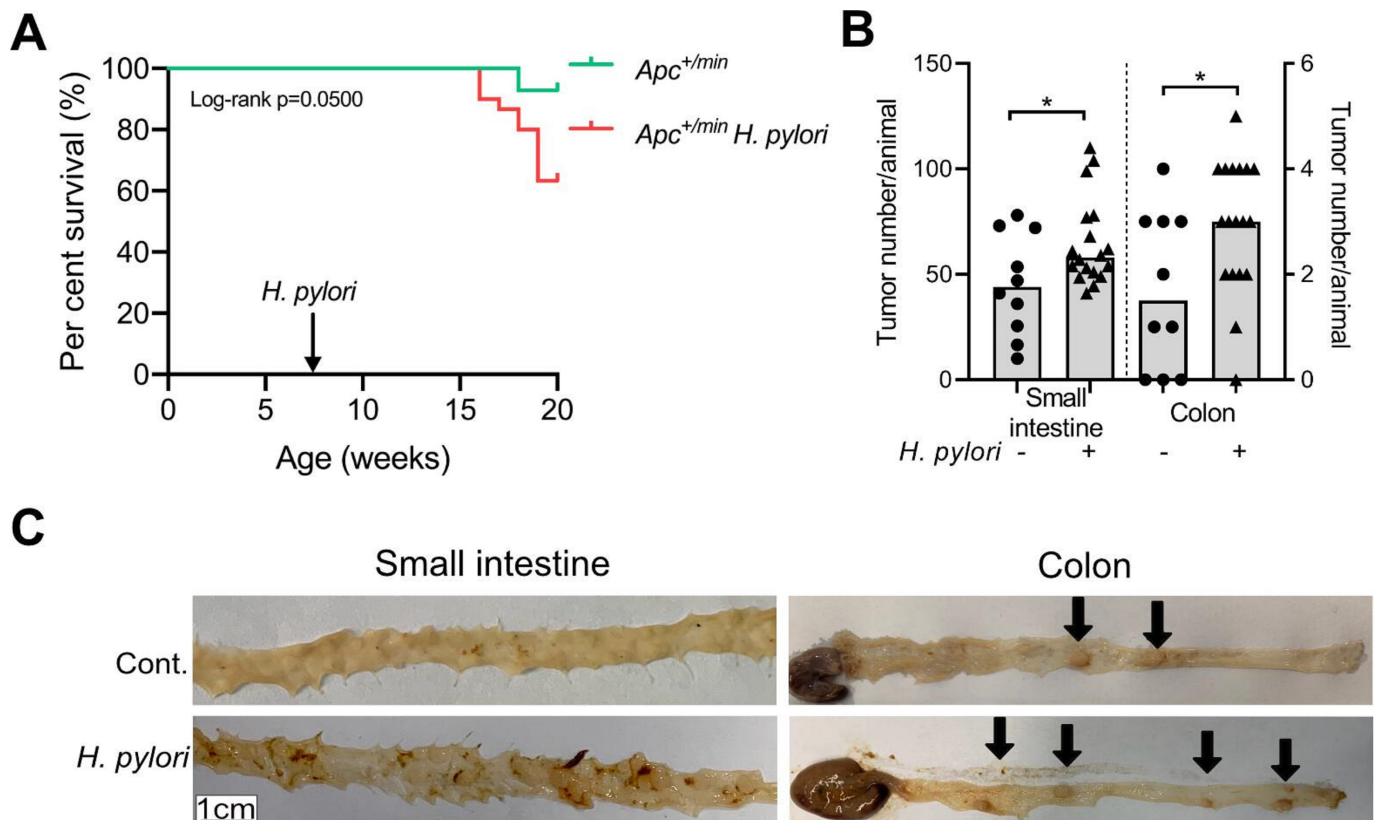


**Figure 1** *Helicobacter pylori* promotes intestinal carcinogenesis in *Apc* mouse models. (A) Kaplan-Meier survival curve comparing *H. pylori*-infected and non-infected *Apc*<sup>+/*min*</sup> mice. (B) Tumour counts of *H. pylori*-infected (n=18) and non-infected (n=10) *Apc*<sup>+/*min*</sup> mice in small intestine and colon. (C) Representative pictures of tumours (arrows) in the small intestine and colon of *H. pylori*-infected and non-infected (controls (Cont.)) *Apc*<sup>+/*min*</sup> mice. Each symbol represents one animal, from three independent, pooled experiments. Bars denote median. Statistical significance was determined with Mann-Whitney U test or unpaired t-test, \*p<0.05.

contributing to gastric carcinogenesis. To assess whether alterations in intestinal immunity could be related to the increased tumour burden observed in infected *Apc* mutant mice, we first analysed lymphocyte infiltration in the small intestine of *Apc*<sup>+/<sup>min</sup> and *Apc*<sup>+/<sup>1638N</sup> mice upon infection (online supplemental figure 1A). Recruitment of intraepithelial CD3<sup>+</sup> T cells to small intestine and colon was increased upon *H. pylori* infection (figure 2A and online supplemental figure 2A), which was also confirmed by flow cytometric analysis of T cells (online supplemental figure 2B,C). Furthermore, this revealed a shift towards more CD8<sup>+</sup> and less CD4<sup>+</sup> T cells upon infection (online supplemental figure 2D). In addition, the abundance and protein level of Foxp3<sup>+</sup> Treg cells was reduced in the small intestine from infected mice compared with uninfected controls, as detected by flow cytometry (figure 2B and online supplemental figure 2E).</sup></sup>

To further explore the underlying mechanisms promoting intestinal tumourigenesis upon *H. pylori* infection independently from tumour-prone backgrounds, we infected wild-type C57BL/6 mice (WT) for 24 weeks and analysed immune responses (online supplemental figure 2F). An increased number of intraepithelial CD3<sup>+</sup> T cells was also observed in the small intestine as well as in the colon of *H. pylori*-infected WT mice compared with uninfected controls (figure 2C). Contrasting the balanced immune phenotype observed in the stomach (figure 2C and online supplemental figure 2G), this was accompanied by a reduction in Foxp3<sup>+</sup> Treg cells (figure 2D and online supplemental figure 2G). Multiplexed ChipCytometry corroborated an overall reduction of Treg cells, and additionally revealed their compartmentalisation within the lamina propria in infected colonic tissue (figure 2E).

We next confirmed the specificity of these T cells for *H. pylori* by restimulating lamina propria CD4<sup>+</sup> T cells with *H. pylori* lysate and measuring the release of the pro-inflammatory cytokine IL-17A, which has been previously described to be one of the main players in the immune response to *H. pylori*.<sup>1</sup> A specific IL-17A/CD4<sup>+</sup> T cell response was observed in infected C57BL/6 and *Apc*<sup>+/<sup>min</sup> mice (online supplemental figure 2H).</sup>

To characterise in depth the specific intestinal immune response elicited by gastric *H. pylori*, we investigated the immune cell compartment on a single cell level by performing 10X single-cell RNA sequencing (scRNAseq) (dataset).<sup>14</sup> We isolated and sorted single CD45<sup>+</sup> immune cells of intestinal and colonic tissue from *Apc*<sup>+/<sup>min</sup> mice and littermate WT controls that had been infected for 12 weeks with *H. pylori*, and compared them with non-infected controls (online supplemental figure 2I).</sup>

Unsupervised clustering identified 16 clusters according to their transcriptional profiles, which are visualised using Uniform Manifold Approximation and Projection (UMAP)<sup>15</sup> (figure 2F and online supplemental figure 2J) and were annotated based on known marker genes (online supplemental figure 2K).

To further characterise the Treg cell compartment, we subclustered and annotated Treg cells, which resulted in three subclusters: activated Treg cells (act. Tregs); peripherally derived Treg cells (pTregs), characterised by high RORγt expression and thymus-derived Treg cells (tTregs), characterised by GATA3 expression<sup>16 17</sup> (figure 2G and online supplemental figure 2L). We then computed a Treg effector score<sup>18</sup> (figure 2H and online supplemental figure 1), and found significantly increased Th17 differentiation genes in infected act. Tregs (figure 2H and online supplemental table 1), indicating that *H. pylori* infection reprogrammes Treg cells into potentially pathogenic Foxp3<sup>+</sup> IL-17A<sup>+</sup> T cells.

Finally, to understand cell dynamics of T cells in infected mice, we calculated RNA velocity vectors, which predict future

states of individual cells based on ratios of spliced and unspliced messenger RNAs.<sup>19</sup> In line with our previous findings, when looking at the CD4 clusters, it was apparent that less CD4 cells were projected towards CD4 Treg cells in infected *Apc* mice (online supplemental figure 2M).

In summary, our results show that *H. pylori* infection induces a *H. pylori*-specific pro-inflammatory immune response in the small intestine and colon of infected mice, that is characterised by loss of Treg cells and their differentiation into Foxp3<sup>+</sup> IL-17A<sup>+</sup> T cells.

### Activation of carcinogenic signalling pathways and loss of goblet cells characterise the intestinal epithelial response to *H. pylori* infection

Considering the alterations induced by *H. pylori* in intestinal immune cells independently of adenomatous polyposis coli (APC) mutations in WT mice, we analysed the effect on signalling pathways putatively mediating the pro-carcinogenic effects of *H. pylori* infection in the epithelium. Therefore, we assessed transcriptomic profiles of EPCAM<sup>+</sup> epithelial cells from *Apc*<sup>+/<sup>min</sup> mice in our scRNAseq data (online supplemental figure 2I) (dataset).<sup>14</sup> Unsupervised clustering revealed 15 clusters according to their transcriptional profiles, which were visualised as UMAP (figure 3A and online supplemental figure 3A) and annotated based on known marker genes (online supplemental figure 3B).</sup>

Pseudo-spatial distribution of epithelial cells along the crypt-villus axis were computed to confirm correct annotation of cell types<sup>20 21</sup> (online supplemental figure 3C).

Here, we specifically explored signalling pathways associated with CRC initiation and development, namely STAT3 and NF-κB. Notably, these pathways also orchestrate key inflammatory mechanisms in inflammation-driven colon cancer and have been extensively related to *H. pylori* infection.<sup>22–24</sup> We computed a score of genes involved in the Jak-STAT signalling pathway, which revealed significantly higher scores in enterocytes of WT and *Apc*<sup>+/<sup>min</sup> mice upon *H. pylori* infection (figure 3B, online supplemental figure 3D and online supplemental table 1). Increased STAT3 signalling was only detected in stem cells of WT mice and not in *Apc*<sup>+/<sup>min</sup> mice upon *H. pylori* infection (online supplemental figure 3D), which can be linked to the binary role of STAT3 in tumourigenesis and a reduced availability of STAT3-inducing receptors during tumour progression, as we found a decreased expression of the IL-22 receptor *Il22ra1* on stem cells of *Apc* mutant mice upon *H. pylori* infection, but not in infected wt mice or in enterocytes (online supplemental figure 3E). When assessing NF-κB signalling in enterocytes, higher scores were observed upon *H. pylori* infection (online supplemental figure 3F and online supplemental figure 1).</sup></sup>

As it has been shown that activation of epithelial STAT3 favours recruitment of lymphocytes, while inhibiting infiltration of Treg cells in the colon,<sup>25</sup> we confirmed hyperactivation of STAT3 in tissue samples from 24 weeks infected *H. pylori* WT (figure 3C) and *Apc* mutant mice (online supplemental figure 1A, figure 3D), which was accompanied by enhanced proliferation as detected by Ki67 staining (figure 3C).

Given that a functional intestinal barrier is depending on mucus replenishment by goblet cells, we next assessed their status by periodic acid-Schiff (PAS) staining. We observed reduced number of mucus producing cells in the small intestine and in the colon of *H. pylori*-infected WT (figure 3C) and *Apc* mutant mice (figure 3E) compared with uninfected controls.



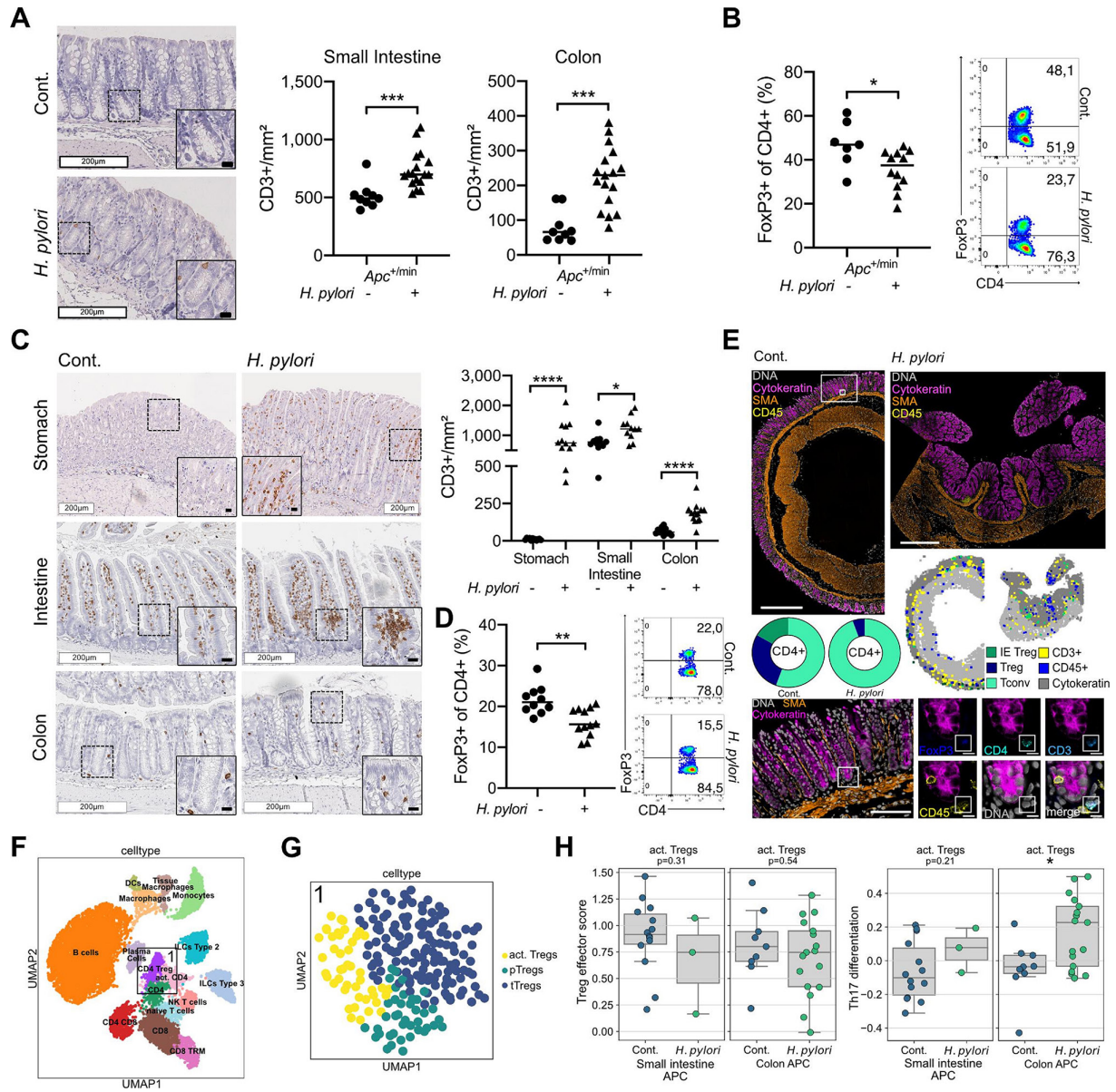


**Figure 2** *Helicobacter pylori* infection induces a pro-inflammatory response in the intestine. (A) Representative pictures of colonic CD3<sup>+</sup> stainings of *H. pylori*-infected and non-infected *Apc*<sup>+/-min</sup> mice after 12 weeks of infection are shown. Squares highlight zoom in. White scale bars correspond to 200  $\mu$ m, black scale bars to 20  $\mu$ m. Quantification of positive cells per mm<sup>2</sup> small intestine and colon tissue is shown. Pooled data of three independent experiments. (B) Flow cytometric analysis of intestinal lamina propria lymphocytes isolated from *H. pylori*-infected and non-infected *Apc*<sup>+/-min</sup> mice after 12 weeks of infection. Frequency of FoxP3<sup>+</sup> cells of CD4<sup>+</sup> T cells are shown, gated on live, single cells, CD45<sup>+</sup> and CD3<sup>+</sup>. Pooled data of two independent experiments. (C) Representative CD3<sup>+</sup> staining of stomach, small intestine and colon tissue sections of *H. pylori*-infected and non-infected C57BL/6 mice after 24 weeks of infection. Quantification of intraepithelial cells per mm<sup>2</sup> is shown. Squares highlight zoom in. White scale bars correspond to 200  $\mu$ m, black scale bars to 20  $\mu$ m. Pooled data of two independent experiments. (D) Frequency of FoxP3<sup>+</sup> cells of CD4<sup>+</sup> T cells are shown. Cells were gated on live, single cells, CD45<sup>+</sup> and CD3<sup>+</sup>. Pooled data of two independent experiments. (E) Overview of colon tissue stained with multiplexed chip cytometry. Automatic image processing of multiplexed chip cytometry on colon tissue determines CD4<sup>+</sup> T cell properties in *H. pylori*-positive and *H. pylori*-negative C57BL/6 mice. Frequencies of conventional T cells (Tconv), regulatory T cells (Treg) and intraepithelial regulatory T cells (IE Treg) are shown. Scale bar in overview corresponds to 500  $\mu$ m. Representative picture of colon tissue stained with multiplexed chip cytometry. FoxP3<sup>+</sup> cell, defined by intranuclear FoxP3<sup>+</sup>, CD4<sup>+</sup>CD3<sup>+</sup> and CD45<sup>+</sup> staining. Large scale bar corresponds to 100  $\mu$ m, small scale bars to 10  $\mu$ m. Representative data of one experiment. (F) Annotated immune cells plotted as Uniform Manifold Approximation and Projection (UMAP), clusters for further analysis are highlighted (1=CD4<sup>+</sup> Treg, 2=CD8 and CD8 TRM). (G) Unsupervised clustering and annotation of Treg cluster as UMAP, n=217 cells. act. Tregs, activated Tregs; pTregs, peripherally induced Tregs; tTregs, thymically derived Tregs. (H) Gene set score of Treg effector genes and Th17 differentiation genes, comparing activated Treg cells from small intestine and colon of *H. pylori*-infected and non-infected *Apc*<sup>+/-min</sup> (APC) mice. Statistical significance was determined with Kruskal-Wallis test. Each symbol represents one animal/single cell, pooled from at least two independent experiments (n=6–10 mice/group/experiment) or two mice/group for single-cell data. Bars denote median. Unless otherwise specified, statistical significance was determined with Student's t-test in case of normal distribution, otherwise by Mann-Whitney U test, \*p<0.05, \*\*p<0.01, \*\*\*p<0.001, \*\*\*\*p<0.0001.



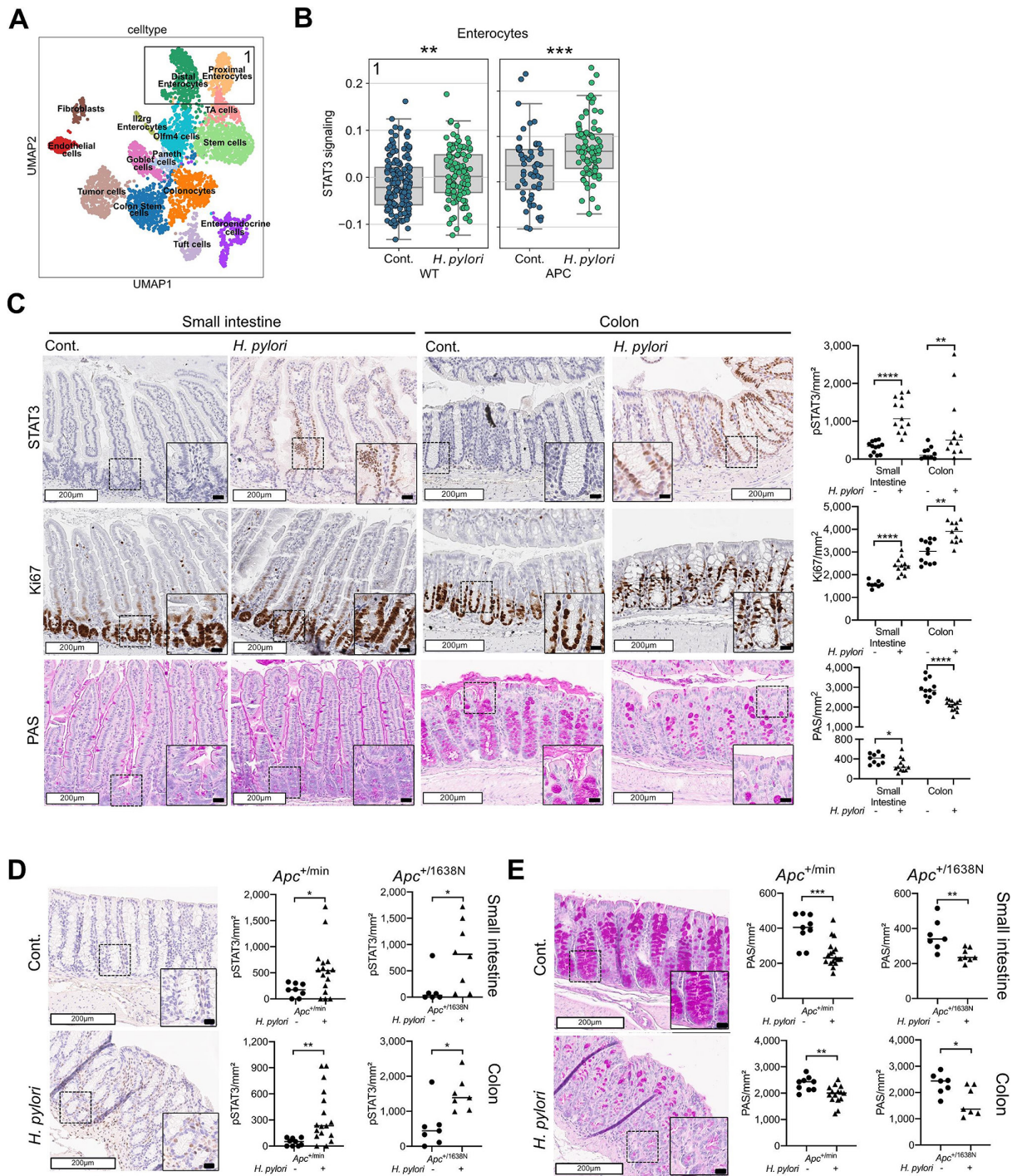


**Figure 3** Activation of carcinogenic signalling pathways and loss of goblet cells characterise the intestinal epithelial response to *Helicobacter pylori* infection. (A) Annotated epithelial cells after unsupervised clustering plotted in Uniform Manifold Approximation and Projection (UMAP) space, n=2 mice per group, n=4249 cells. Clusters for further analysis are highlighted (1=enterocytes). (B) Gene set score of STAT3 signalling genes, comparing intestinal enterocytes from *H. pylori*-infected and non-infected *Apc*<sup>+/+</sup> (WT) and *Apc*<sup>+/-min</sup> (APC) mice. Statistical significance was determined with Kruskal-Wallis test. (C) Representative pSTAT3, Ki67 and periodic acid-Schiff (PAS) staining of small intestine and colon tissue of *H. pylori*-infected and non-infected C57BL/6 mice. Quantification of positive cells per mm<sup>2</sup> is shown. Squares highlight zoom in. White scale bars correspond to 200 μm, black scale bars to 20 μm. Pooled data of two independent experiments. (D) Representative pictures of colonic pSTAT3 staining of *H. pylori*-infected and non-infected *Apc*<sup>+/-min</sup> and *Apc*<sup>+/-1638N</sup> mice are shown. Squares highlight zoom in. White scale bars correspond to 200 μm, black scale bars to 20 μm. Quantification of positive cells per mm<sup>2</sup> are shown. Pooled data of three independent experiments. (E) Representative pictures of colonic PAS staining of *H. pylori*-infected and non-infected *Apc*<sup>+/-min</sup> and *Apc*<sup>+/-1638N</sup> mice are shown. Squares highlight zoom in. White scale bars correspond to 200 μm, black scale bars to 20 μm. Quantification of positive cells per mm<sup>2</sup> are shown. Pooled data of three independent experiments. Each symbol represents one animal/single cell, pooled from at least two independent experiments (n=6–10 mice/group/experiment) or two mice/group for single-cell data. Bars denote median. Unless otherwise specified, statistical significance was determined with Student's t-test in case of normal distribution, otherwise by Mann-Whitney U test, \*p<0.05, \*\*p<0.01, \*\*\*p<0.001, \*\*\*\*p<0.0001.

To explore in depth the effects of *H. pylori* infection on the goblet cells, we clustered and annotated goblet cells in our scRNAseq dataset based on goblet cell differentiation markers.<sup>26</sup> This revealed immature, characterised by high expression of *Tff3*; intermediate, highly expressing *Oasis* and terminal goblet cells, with high expression of *Muc2* and *Klf4* (online supplemental figure 3G,H). Maturation states were distinctly affected by *H. pylori* infection, with a switch to less differentiated goblet cells (online supplemental figure 3I). To assess goblet cell functionality, we assessed the expression of genes encoding for antimicrobial peptides *Reg3b* and *Reg3g*, which are known to play a role in response to pathogens and inflammation<sup>27</sup> (online supplemental table 1). We found them to be reduced upon *H. pylori* infection (online supplemental figure 3J). As those genes are known to be downstream targets of STAT3, we checked for STAT3 signalling specifically in the goblet cell cluster, which was—in contrast to the increased STAT3 signalling in enterocytes and stem cells—not induced upon *H. pylori* infection (online supplemental figure 3K). These findings are consistent with a compromised intestinal barrier integrity induced by *H. pylori* infection, independent of *APC* status.

To explain the absolute loss of goblet cells we observed in infected mice, we studied cellular dynamics of goblet cells by means of RNA velocities. In the colon, we observed less directionality from the stem cell cluster towards the goblet cell cluster, and at the same time a higher projection towards the colonocyte cluster upon *H. pylori* infection (online supplemental figure 3J), in contrast to the small intestinal goblet cell cluster, where cell dynamics seem to be restricted to the goblet cell cluster itself. When assessing the expression of *Atoh1*, which is known to drive terminal differentiation into the secretory lineage,<sup>28</sup> in stem cells of both small intestine and colon, a significantly lower expression was found upon *H. pylori* infection (online supplemental figure 3K). These findings indicate a skewed differentiation of stem cells rather into unspecialised colonocytes than into goblet cells.

Together, these results indicate that *H. pylori* induces carcinogenic signalling pathways and has a detrimental impact on mucus-producing goblet cells in the small intestine and colon of WT and *Apc* mutant mice.

### ***H. pylori* infection favours the presence of mucus-degrading microbiota and shapes a pro-inflammatory and pro-carcinogenic microbiota signature**

Microbiota alterations and aberrant presence of certain bacterial species in the small intestine have been related to the development of CRC.<sup>29</sup> This could be an additional mechanism by which *H. pylori* contributes to intestinal carcinogenesis, since *H. pylori* infection has been shown to alter microbiota signatures.<sup>30</sup> Therefore, we assessed to which extent *H. pylori* infection influenced small intestinal and colonic microbial composition by performing 16S RNA sequencing (dataset).<sup>14</sup> While we found significantly increased abundance of *Helicobacter* spp in the stomach of 24 weeks infected mice, we did not detect *H. pylori* in intestine and colon (online supplemental figure 4A). When comparing the microbiota in caecum and colon of infected and non-infected mice via taxonomic profiling, we observed apparent changes at phylum level upon *H. pylori* infection (figure 4A). Furthermore, we found signs of decreased  $\alpha$ -diversity in small intestine upon *H. pylori* infection (online supplemental figure 4B) as well as significantly different  $\beta$ -diversity in caecum, stool and small intestine between non-infected and infected mice (online supplemental figure 4C). Differential abundance testing revealed

*Akkermansia* spp to be enriched in 24 weeks infected WT mice (online supplemental figure 4D, figure 4B). When exploring the data for further species sharing the mucus-degrading characteristics of *Akkermansia* spp, we found an increase in *Ruminococcus* spp (figure 4B and online supplemental figure 4D). The abundance of both species was also higher in *Apc* mutant mice (online supplemental figure 1A) upon *H. pylori* infection (figure 4C,D).

To determine the functional effects of *H. pylori*-induced microbiota signatures independent of mutant *APC*, we performed a stool transfer experiment from infected and non-infected specific pathogen-free (SPF) mice into germ-free WT mice (online supplemental figure 4E). This revealed an increased T-cell infiltration into intestinal and colonic epithelia (figure 4E and online supplemental figure 4F), a reduction of Foxp3<sup>+</sup> Treg cells (figure 4F) and lower amounts of ROR $\gamma$ t<sup>+</sup> Treg cells (figure 4G), which are known to be microbiota-induced,<sup>31</sup> in WT stool recipients from *H. pylori*-infected mice. Furthermore, we observed enhanced STAT3 signalling in intestines of WT mice that received stool from *H. pylori*-infected mice (figure 4H and online supplemental figure 4G). In order to ultimately assess the contribution of *H. pylori*-induced changes in microbiota to intestinal carcinogenesis, we performed a further stool transfer experiment from SPF non-infected and *H. pylori*-infected *Apc*<sup>+1638N</sup> mice and WT littermates into germ-free *Apc*<sup>+1638N</sup> mice (online supplemental figure 4H). Higher tumour numbers in stool recipients from *H. pylori*-infected mice were found, which was already evident in WT mice and further enhanced in an *Apc*<sup>+1638N</sup> background (online supplemental figure 4I).

Together, *H. pylori* alters the microbiota of the lower GI tract, favours mucus-degrading microbiota in both WT and *Apc* mutant mice and induces a pro-inflammatory and pro-carcinogenic microbiota signature.

### ***H. pylori*-induced colorectal carcinogenesis is prevented by eradication**

The interplay between a pro-inflammatory response and activation of pro-carcinogenic signalling, accompanied by alterations in microbiota characterised *H. pylori*-driven intestinal tumourigenesis. To dissect the contribution of inflammation in the absence of microbiota, we infected *Apc*<sup>+1638N</sup> mice under germ-free conditions (online supplemental figure 5A,B). We observed similar immune alterations as in SPF mice, namely increased CD3<sup>+</sup> T cell infiltration and reduction of Treg cells in small intestine and colon (figure 5A, online supplemental figure 5E,B). In contrast, germ-free mice barely showed activation of STAT3 signalling, and no reduction of goblet cells upon *H. pylori* infection (online supplemental figure 5C–E). Importantly, we did not observe significant differences in tumour number between control and *H. pylori*-infected germ-free *Apc*<sup>+1638N</sup> mice (figure 5C), which, in combination with our findings from stool transfer experiments (figure 4 and online supplemental figure S4), indicates a strong contribution of *H. pylori*-induced changes in microbiota to the tumour phenotype, and suggests, that *H. pylori*-induced carcinogenesis in the small intestine and colon is a multifactorial process involving the interplay of the pro-inflammatory immune response, alterations in microbiota and pro-carcinogenic signalling. Therefore, we next sought to determine whether eradication of *H. pylori* infection could abrogate the carcinogenic process, by treating the mice with a triple therapy regimen consisting of clarithromycin, metronidazole and omeprazole,<sup>32</sup> reflecting the ‘Italian triple therapy’ regimen also used in infected patients to eradicate *H. pylori* (figure 5D and online supplemental figure 5F). Importantly, we



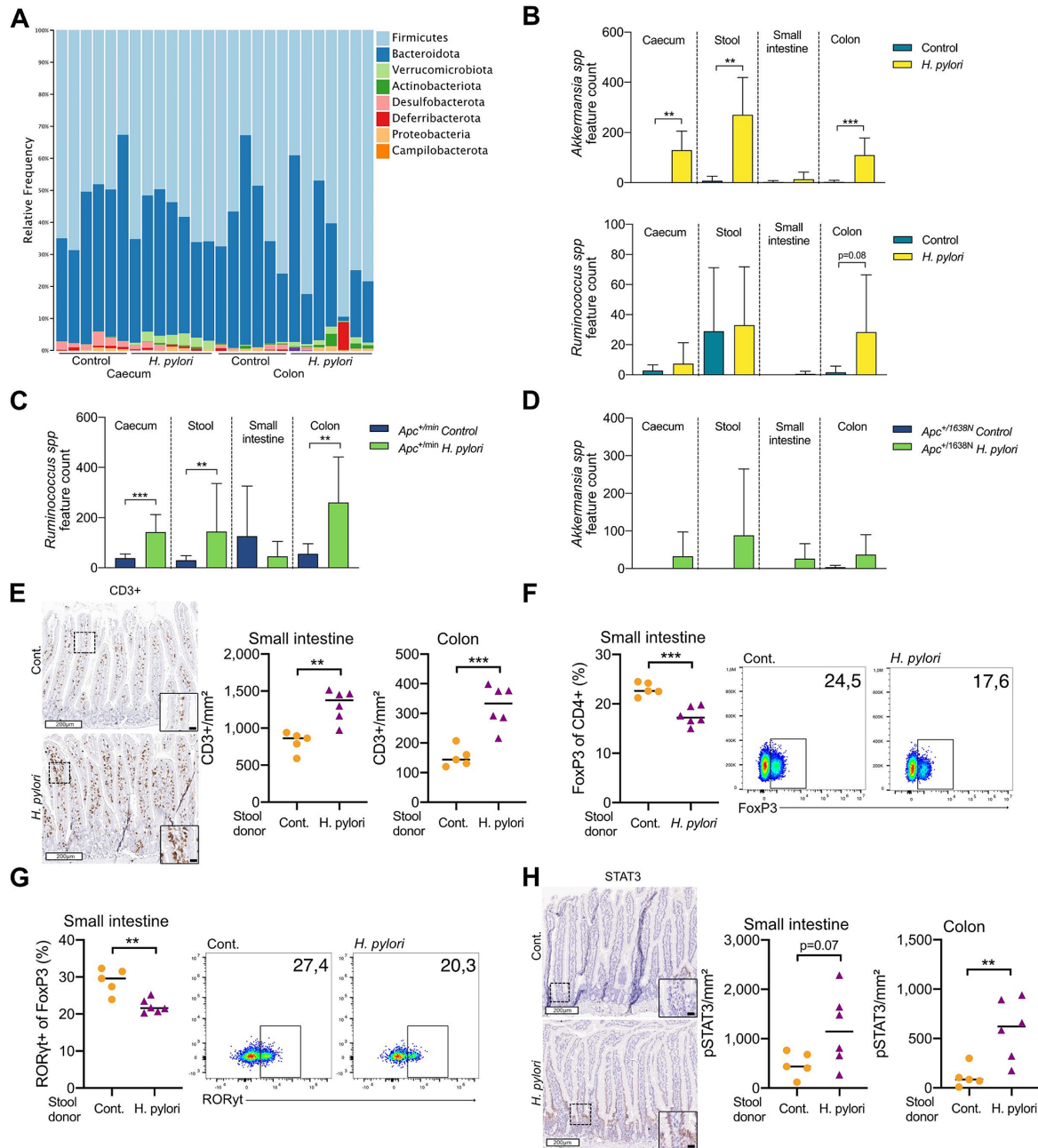


**Figure 4** *Helicobacter pylori* infection favours the presence of mucus-degrading microbiota and shapes a pro-inflammatory and pro-carcinogenic microbiota signature. (A) Relative taxonomic frequencies on phyla level in 16S rRNA sequenced caecum and colon samples of *H. pylori*-infected and non-infected C57BL/6 mice (n=6–8 mice/group). Data of one representative experiment of two to three independent experiments. (B) Feature counts of Amplicon Sequence Variants (ASVs) of *Akkermansia* spp and *Ruminococcus* spp in caecum, stool, small intestine and colon of *H. pylori*-infected and non-infected C57BL/6 mice (n=6–8 mice/group). Data of one representative experiment of two to three independent experiments. (C) Feature counts (ASVs) of *Ruminococcus* spp of caecum, stool, small intestine and colon of *H. pylori*-infected and non-infected *Apc*<sup>+/*min*</sup> mice (n=4–5 mice/group). Data of one representative experiment of two to three independent experiments. (D) Feature counts (ASVs) of *Akkermansia* spp of caecum, stool, small intestine and colon of *H. pylori*-infected and non-infected *Apc*<sup>+/*1638N*</sup> mice (n=4–5 mice/group). Data of one representative experiment of two to three independent experiments. (E) Representative pictures of intestinal CD3+ stainings of germ-free wild-type (WT) mice receiving stool transfer from *H. pylori*-infected (*H. pylori*) and non-infected (*Cont.*) WT mice analysed 12 weeks after transfer are shown. Squares highlight zoom in. White scale bars correspond to 200 µm, black scale bars to 20 µm. Quantification of positive cells per mm<sup>2</sup> small intestine and colon tissue is shown. Data of one experiment. (F) Flow cytometric analysis of intestinal lamina propria lymphocytes isolated from germ-free WT mice receiving stool transfer from *H. pylori*-infected (*H. pylori*) and non-infected (*Cont.*) WT mice analysed 12 weeks after transfer. Frequency of FoxP3+ cells of CD4+ T cells and (G) RORγt+ cells of FoxP3+ T cells are shown, gated on live, single cells, CD45+, CD3+ and CD4+. Data of one experiment. (H) Representative pictures of intestinal STAT3+ stainings of germ-free WT mice receiving stool transfer from *H. pylori*-infected (*H. pylori*) and non-infected (*Cont.*) WT mice analysed 12 weeks after transfer are shown. Squares highlight zoom in. White scale bars correspond to 200 µm, black scale bars to 20 µm. Quantification of positive cells per mm<sup>2</sup> small intestine and colon tissue is shown. Data of one experiment. Data shown as bars with mean and SD or each symbol represents one animal (n=5–6 mice/group). Bars denote median. Statistical significance was determined with Student's t-test in case of normal distribution, otherwise by Mann-Whitney U test, \*\*p<0.01, \*\*\*p<0.001.



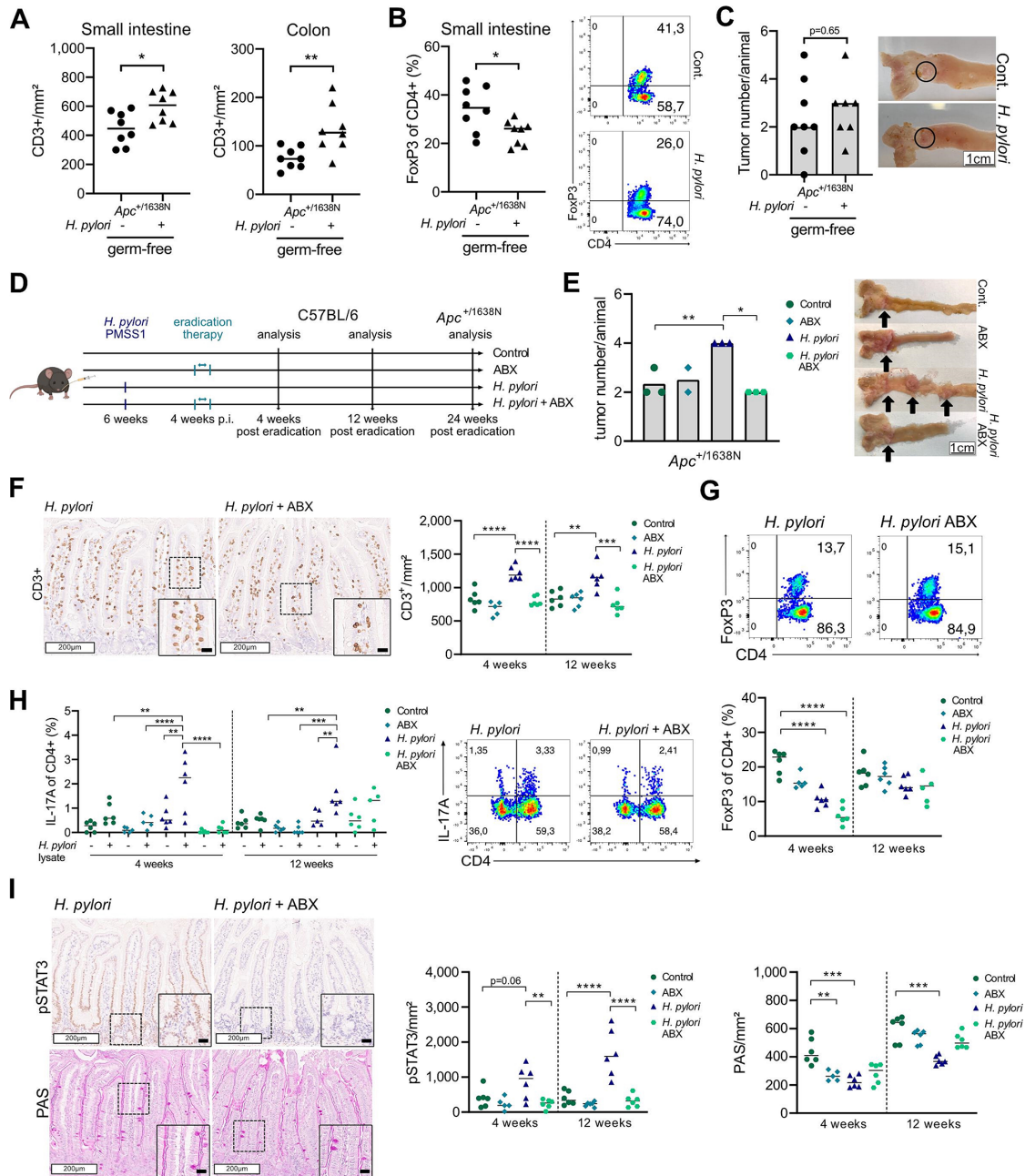


**Figure 5** *Helicobacter pylori*-induced intestinal carcinogenesis is prevented by eradication. (A) Quantification of small intestinal and colonic intraepithelial CD3<sup>+</sup> cells per mm<sup>2</sup> of *H. pylori*-infected and non-infected germ-free  $Apc^{+/1638N}$  mice is shown. Pooled data of two independent experiments ( $n=8$  mice/group). (B) Frequencies of FoxP3<sup>+</sup> cells of CD4<sup>+</sup> T cells, gated on live, single cells, CD45<sup>+</sup> and CD3<sup>+</sup> of *H. pylori*-infected and non-infected germ-free  $Apc^{+/1638N}$  mice are included. Representative pseudo-colour plots are shown. Pooled data of two independent experiments ( $n=8$  mice/group). (C) Intestinal tumour counts of *H. pylori*-infected and non-infected germ-free  $Apc^{+/1638N}$  mice and representative pictures of tumours (circled) are shown ( $n=8$  mice/group). (D) Experimental setup of *H. pylori* eradication therapy of C57BL/6 and  $Apc^{+/1638N}$  mice. (E) Tumour counts of non-infected, antibioticly treated, *H. pylori*-infected and *H. pylori*-eradicated  $Apc^{+/1638N}$  mice and representative pictures of tumours in the small intestine. Data of one experiment ( $n=2-3$  mice/group). (F) Representative pictures of CD3<sup>+</sup> stainings from small intestinal tissue of *H. pylori*-infected and *H. pylori*-eradicated C57BL/6 mice are shown. Squares highlight zoom in. White scale bars correspond to 200  $\mu$ m, black scale bars to 20  $\mu$ m. Quantification of positive cells per mm<sup>2</sup> is shown. Data of one experiment ( $n=5-6$  mice/group). (G) Flow cytometric analysis of intestinal lamina propria lymphocytes reveals frequency of FoxP3<sup>+</sup>CD4<sup>+</sup> T cells, gated on live, single cells, CD45<sup>+</sup> and CD3<sup>+</sup>. Data of one experiment ( $n=5-6$  mice/group). (H) Flow cytometric analysis of intestinal lamina propria lymphocytes reveals IL-17A release of CD4<sup>+</sup> T cells, restimulated with whole *H. pylori* lysate. Cells are gated on live, single cells, CD45<sup>+</sup> and CD3<sup>+</sup>. Data of one experiment ( $n=5-6$  mice/group). (I) Representative pictures of pSTAT3 and periodic acid-Schiff (PAS) staining from intestinal tissue of *H. pylori*-infected and *H. pylori*-eradicated C57BL/6 mice are shown. Squares highlight zoom in. White scale bars correspond to 200  $\mu$ m, black scale bars to 20  $\mu$ m. Quantification of positive cells per mm<sup>2</sup> is shown. Data of one experiment ( $n=5-6$  mice/group). Each symbol represents one animal. Bars denote median. Statistical significance between two groups was determined with Student's t-test in case of normal distribution and otherwise with Mann-Whitney U test. Among more than two groups, ordinary one-way analysis of variance with Tukey's multiple comparisons test was applied in case of normal distribution, otherwise Kruskal-Wallis test with Dunn's multiple comparisons test, \* $p<0.05$ , \*\* $p<0.001$ .

found that after antibiotic eradication, tumour burden was at the same levels as in uninfected controls (figure 5E). To delineate that the underlying changes in the intestinal immune response were directly induced by *H. pylori* infection and independent of mutated *Apc*, we analysed the effect of *H. pylori* eradication on C57Bl/6 mice (figure 5D and online supplemental figure 5F), and found a lower CD3<sup>+</sup> T cell infiltration in the stomach (online supplemental figure 5G), small intestine and colon (figure 5F, online supplemental figure 5E) compared with infected mice at 4 and 12 weeks post-eradication. The percentage of Treg cells was initially reduced in eradicated mice 4 weeks after treatment, while 12 weeks post-treatment, the percentage of FoxP3<sup>+</sup> T cells was observed to recover (figure 5G). A specific IL-17A/CD4<sup>+</sup> T cell response was observed in infected mice, which was initially lost after eradication therapy, but then reappeared after longer recovery time (figure 5H), supporting the specificity of the response to *H. pylori*, based on the given antigen encounter and response also in eradicated mice. Importantly, the clearance of infection resulted in normalisation of STAT3 activation and the number of PAS-positive cells (figure 5I and online supplemental figure 5H), confirming that *H. pylori* is specifically responsible for these changes.

In summary, our results demonstrate that *H. pylori* directly enhances colon carcinogenesis by shaping intestinal and colonic immune responses and inducing profound changes in intestinal/colonic microbiota and epithelial homeostasis. Eradication of *H. pylori* infection prevents its tumour-promoting effects also in the colon, providing a possible additional strategy to reduce CRC burden.

### *H. pylori* alters colonic homeostasis in human

Our mouse models showed that *H. pylori* affects intestinal and colonic homeostasis at different cellular and molecular levels, which can ultimately enhance tumour development. To determine whether these effects were also observed in humans, we analysed immune signatures in a cohort of 154 human colon tissue samples (online supplemental table 2). Based on immune responses and histology of the stomach, we stratified samples according to *H. pylori* status into currently (actively) infected and eradicated patients. We found that *H. pylori*-actively infected as well as eradicated individuals showed higher infiltration of CD3<sup>+</sup> T cells in the colon compared with uninfected subjects (figure 6A). Using endoscopy-derived colon biopsies, we further characterised T cell responses by flow cytometry, which revealed tendencies towards more CD3<sup>+</sup> T cells in the colonic mucosa of currently infected patients (online supplemental figure 6A). In contrast, CD4<sup>+</sup> and CD8<sup>+</sup> subsets were not affected by *H. pylori* status (online supplemental figure 6B). Notably, the number of FoxP3<sup>+</sup> cells in the colonic mucosa was lowest in the currently infected group, whereas eradicated patients seem to level with negative controls (figure 6C). The overall loss of Tregs was confirmed via ChipCytometry (figure 6B), which additionally showed that intraepithelial localisation of Tregs is almost lost in colon samples from *H. pylori*-infected individuals (figure 6B and online supplemental figure 6C).

We next focused on the epithelial compartment and, in concordance with our findings in mice and our eradication experiments, found a higher number of pSTAT3-positive epithelial cells and a concomitant loss of mucus-producing cells in the colon of currently infected subjects, which was attenuated in eradicated patients (figure 6A).

Finally, we assessed microbial changes in stool of patients and found a difference in  $\beta$ -diversity between actively *H. pylori*-infected and *H. pylori*-negative patients ( $p=0.062$ ), but not between *H. pylori*-eradicated and *H. pylori*-negative patients

( $p=0.552$ ) (figure 6D). In contrast, we neither detected significant changes in  $\alpha$ -diversity (online supplemental figure 6D) nor in Firmicutes-to-Bacteroidetes ratio (online supplemental figure 6E) between the three groups. Comparative microbiome profiling revealed Prevotellaceae and Peptostreptococcales, which have been associated with CRC, to be differentially abundant in *H. pylori*-positive patients (online supplemental figure 6F,G).

These results confirm that the immune and epithelial signatures identified in mouse models upon *H. pylori* infection are also observed in humans, and are accompanied by changes in microbiota compositions, which can further contribute to colon carcinogenesis. Furthermore, the attenuated phenotype observed in *H. pylori*-eradicated patients further supports *H. pylori* status as an independent risk factor for CRC and simultaneously offers an option for CRC prevention for those patients at risk.

### DISCUSSION

Although selectively colonising the stomach, chronic *H. pylori* infection is associated with several extragastric diseases.<sup>33</sup> Epidemiological data indicate an association between *H. pylori* infection and a higher risk and aggressiveness of CRC, with an OR of 1.9,<sup>34</sup> an OR higher than for most other known risk factors, such as smoking, alcohol and body mass index.<sup>34</sup> However, these epidemiological data have not yet been confirmed experimentally, and a molecular mechanism by which *H. pylori* may promote CRC remained elusive. We employed *Apc* mutant mouse lines (*Apc*<sup>+/<sup>min</sup> and *Apc*<sup>+/<sup>1638N</sup>) as surrogate models for human CRC, and observed a nearly twofold increase in tumour numbers in mice infected with *H. pylori*, which coincides with the OR observed in epidemiological studies. Remarkably, this increase was observed in the small intestine, where both models usually show most tumours, and was especially evident in the colon. This prompted us to decipher the potential mechanisms driving *H. pylori*-induced carcinogenesis in the small intestine and colon.</sup></sup>

The effects of *H. pylori* infection on other organs are best understood for the lung, where chronic *H. pylori* infection imposes a regulatory immune signature that protects from asthma disease.<sup>35</sup> In contrast to these observations, we observed an *H. pylori* antigen-specific pro-inflammatory Th17-mediated response in the small intestine and colon, which was not balanced by an increase in Treg cells, as it occurs in the stomach or lung. The immune response mounted towards *H. pylori* originates from Peyer's patches in the gut,<sup>2</sup> which may explain why *H. pylori*-specific T cells also homed to intestinal and colonic mucosal sites. Interestingly, IL-17 was found to be increased in *H. pylori*-positive patients with gastritis and gastric cancer,<sup>36</sup> and in CRC, where Th17 signatures, including RORC, IL17, IL23 and STAT3, were linked to poorer prognosis.<sup>37</sup> Still, it was surprising to observe a loss of intestinal Treg cells, which also contrasts the balanced immune response usually observed in the stomach upon *H. pylori* infection. Additionally, we found that in the lower GI tract, Tregs were reprogrammed to upregulate Th17 differentiation markers. Murine and human studies have demonstrated that Treg cells can be reprogrammed to a distinct population, Foxp3<sup>+</sup>/IL17<sup>+</sup> T cells, phenotypically and functionally resembling Th17 cells.<sup>38</sup> Particularly in CRC, the presence of Foxp3<sup>+</sup>/IL17<sup>+</sup> T cells has been reported to be increased in the mucosa and peripheral blood of patients with chronic colitis as well as in colorectal tumours.<sup>39</sup> Foxp3<sup>+</sup>/IL17<sup>+</sup> cells were shown to promote the development of tumour-initiating cells by increasing the expression of several CRC-associated markers



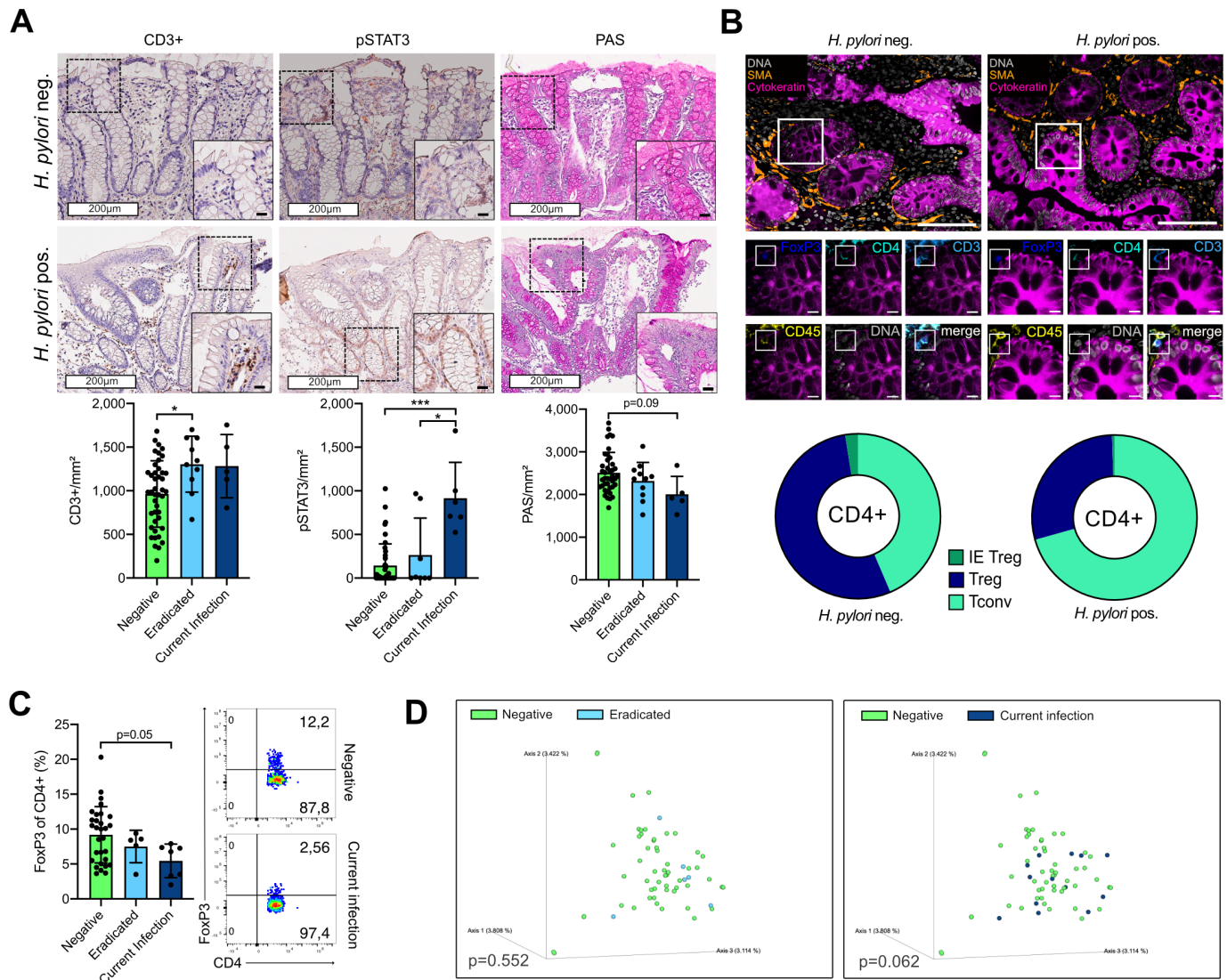


**Figure 6** *Helicobacter pylori* alters colonic homeostasis in human. (A) Representative H&E, CD3+, pSTAT3 and periodic acid-Schiff (PAS) pictures of colonic tissue from *H. pylori* currently infected, eradicated and non-infected patients are shown. Squares highlight zoom in. White scale bars correspond to 200  $\mu$ m, black scale bars to 20  $\mu$ m. Quantification of total CD3+, intraepithelial STAT3 and PAS-positive cells per mm<sup>2</sup> are shown. (B) Representative pictures of human colon tissue stained by multiplexed chip cytometry. FoxP3+ cell, defined by intranuclear FoxP3+, CD4+, CD3+ and CD45+ staining are shown for *H. pylori*-negative and *H. pylori*-positive tissue. Large scale bar corresponds to 100  $\mu$ m, small scale bar to 10  $\mu$ m. Automatic image processing of multiplexed chip cytometry on colon tissue determines CD4+ T cell properties in *H. pylori*-positive and *H. pylori*-negative individuals: frequencies of conventional T cells (Tconv), regulatory T cells (Treg) and intraepithelial regulatory T cells (IE Treg) are shown. (C) Flow cytometric analysis of colon biopsies from *H. pylori* currently infected, eradicated and non-infected patients were conducted. Frequencies of FoxP3+ cells of CD4+ T cells, gated on live, single cells, CD45+ and CD3+ are shown and representative pseudo-colour plots of *H. pylori* currently infected and negative individuals are included. (D) Bray-Curtis dissimilarity depicting  $\beta$ -diversity between *H. pylori*-infected and eradicated as well as *H. pylori*-infected and non-infected patients. Statistical significance was determined with permutational multivariate analysis of variance (PERMANOVA). Each symbol represents one patient, shown as bars with mean and SD. Statistical significance was determined with ordinary one-way analysis of variance with Tukey's multiple comparisons test in case of normal distribution, otherwise by Kruskal-Wallis test with Dunn's multiple comparisons test. \* $P < 0.05$ , \*\* $p < 0.01$ , \*\*\* $p < 0.001$ , \*\*\*\* $p < 0.0001$ .

such as CD44 and epithelial cell adhesion molecule EPCAM in bone marrow-derived mononuclear cells.<sup>40</sup> Thus, the pro-inflammatory Th17 response elicited by *H. pylori*, especially the differentiation of Treg cells to a Th17 phenotype, may constitute one of the major mechanisms enhancing tumour development. This is in line with literature showing that altered T cell homeostasis is a key event during colorectal carcinogenesis, driving tumour development and progression, and determining treatment response of patients with CRC.<sup>41</sup>

Mutations in the gene encoding APC are the most frequent driver mutations leading to sporadic CRC, together with mutations in TP53 and KRAS.<sup>42-43</sup> Pro-inflammatory and proliferative signalling pathways such as STAT3, NF- $\kappa$ B and WNT signalling, activated by signals derived from epithelial and immune cells, drive chronic inflammation, a known mechanism contributing to CRC.<sup>24-44</sup> CRC risk is markedly increased in patients with chronic inflammatory bowel disease, with the risk rising with the duration of disease, from 8.3% after 20 years, to 18.4% after



30 years.<sup>45</sup> Mechanistically, besides immune signalling by Th17 cells, activation of pro-inflammatory signalling pathways as well as altered microbiota, contribute to the pathogenesis of colitis-associated cancer.<sup>46</sup>

The strong pro-inflammatory response induced locally by *H. pylori* in the small intestine was accompanied by the activation of NF- $\kappa$ B and STAT3 pathways. Activation of STAT3 signalling has been strongly related to tumour initiation and development and progression, while levels of activated STAT3 in the tissue correlate with tumour invasion, tumour, node, metastases stage and reduced overall survival of patients with CRC.<sup>47</sup> In addition, the activation of epithelial STAT3 was reported to downregulate the expression of chemokines important for the recruitment of Treg cells in the intestine.<sup>25</sup> Therefore, it is tempting to speculate that during *H. pylori* infection, activation of STAT3 in intestinal and colonic epithelial cells contributes to loss of Treg recruitment, thereby supporting malignant transformation of the intestinal tissue. This central role for STAT3 during carcinogenesis in the intestine is supported by the fact that depletion of STAT3 in *Apc*<sup>+/min</sup> mice led to a reduction in the incidence of early adenomas.<sup>48</sup> Furthermore, in *Apc*<sup>+/min</sup> mice, tumour progression and metastasis were characterised by loss of STAT3 signalling in stem cells due to lower IL-22-receptor expression.<sup>48, 49</sup> We observed similar characteristics in our *H. pylori*-infected mice, indicative of more advanced tumourigenesis.

Importantly, we observed a reduction and normalisation of STAT3 levels after eradication of *H. pylori*, which resulted in a normalisation of tumour load. Notably, for eradication, a treatment regimen also applied in humans was used in order to be able to translate the results to humans.

The function of STAT3 as oncogene or tumour suppressor seems to be determined by the milieu eliciting its activation as well as the local gut microbiota,<sup>50</sup> which is increasingly recognised as an important regulator of colonic cancer development.<sup>51</sup> Interestingly, microbial induction of IL-17A production has been shown to endorse colon cancer initiation and progression in *Apc*<sup>+/min</sup> mice, which was mediated via STAT3 signalling.<sup>52</sup> We thus hypothesised that alterations in microbiota compositions in the intestine and colon induced by *H. pylori* may also contribute to carcinogenesis.<sup>30, 53</sup> Indeed, when housing mice under germ-free conditions, activation of STAT3 and tumour development were lower upon *H. pylori* infection, but not completely normalised, indicating that microbiota alterations are involved in the phenotype but not exclusively responsible.

Such disturbances in gut microbiota communities have been shown to contribute to CRC development and progression.<sup>29</sup> *H. pylori* is known to affect local gastric microbiota, and distant microbial populations in intestine and colon.<sup>30, 54</sup> It has been shown that inflammation-driven dysregulation of microbiota can promote colorectal tumour formation and progression<sup>55</sup> and that in response to bacterial stimuli or pathogen-associated molecular receptors, pro-inflammatory pathways such as c-Jun/JNK and STAT3 signalling pathways are activated and accelerate intestinal tumour growth in *Apc*<sup>+/min</sup> mice.<sup>50</sup> This was supported by our findings from transferring stool of *H. pylori*-infected SPF mice into germ-free mice, which led to lower abundance of FoxP3+ Treg cells and microbiota-induced (FoxP3+ROR $\gamma$ t+) Treg cells as well as STAT3 induction in recipients of stool from *H. pylori*-infected mice, and eventually an accelerated tumour development in comparison to stool transferred from non-infected mice. Together, these data indicate that *H. pylori*-induced pro-inflammatory and pro-carcinogenic microbial signatures are involved in and indispensable to promote intestinal tumour growth.

Our data revealed a distinct mucus-degrading microbiota signature associated with *H. pylori* infection in mice, namely enrichment with *Akkermansia* spp and *Ruminococcus* spp, while in human samples from *H. pylori*-infected patients, bacterial taxa associated with CRC, Prevotellaceae and Peptostreptococcales, were found.<sup>29</sup> Although some studies established an inverse correlation between the presence of *Akkermansia* and GI diseases,<sup>56</sup> *Akkermansia* has been reported to be increased in patients with CRC most likely due to the overexpression of certain mucins in the tumours.<sup>57</sup> Notably, we also observed a general loss of goblet cells, which are important to produce mucins and antimicrobial peptides. This loss of goblet cells was also observed in clinical samples from *H. pylori*-infected patients undergoing colonoscopy. Thus, *H. pylori* infection disrupts, by two distinct mechanisms, intestinal mucus integrity essential to maintain a healthy barrier to impair bacterial penetration. In the absence of a sufficient regulatory T cell response—as observed here—which normally keeps inflammatory signals at bay, the carefully balanced homeostasis maintained in the gut by the interplay of a ‘healthy’ microbiome and an intact mucosa then fails to balance the pro-inflammatory signature elicited by *H. pylori* infection, enabling carcinogenesis. Eradication of *H. pylori* restored intestinal homeostasis with reappearance of goblet cells and normalised the intestinal immune signature, which then completely abrogated the tumour-promoting effect.

Importantly, when analysing colonic biopsies from *H. pylori*-infected patients, we could observe the very same alterations as seen in mice, with activation of pro-carcinogenic signalling pathways and a significant reduction in Treg cells, and an increase of CD3<sup>+</sup> cells. The attenuated phenotype in eradicated patients highlight the clinical relevance of our findings and indicate that *H. pylori* infection is more than a mere risk factor for colon carcinogenesis, but actively promotes a pro-carcinogenic niche in the colon that may be prevented by eradication of *H. pylori*, which therefore could decrease the risk of CRC development in infected individuals. However, studies showing a correlation between *H. pylori* infection and CRC did not address the effect of antibiotic therapy. The inclusion of such cohorts in future studies is important to determine the impact of *H. pylori* eradication in CRC development.

In summary, our study provides solid experimental evidence that *H. pylori* infection accelerates intestinal and colonic tumour development, and offers insight into the underlying mechanisms. We suggest *H. pylori* screening and eradication as a potential measure for CRC prevention strategies.

#### Author affiliations

<sup>1</sup>Institute for Medical Microbiology, Immunology and Hygiene, School of Medicine, Technical University of Munich, Munich, Germany

<sup>2</sup>Boehringer Ingelheim Pharma GmbH & Co. KG, Drug Discovery Sciences, Biberach an der Riß, Germany

<sup>3</sup>Department of Surgery, Klinikum rechts der Isar, School of Medicine, Technical University of Munich, Munich, Germany

<sup>4</sup>Klinik und Poliklinik für Innere Medizin II, Klinikum rechts der Isar, School of Medicine, Technical University of Munich, Munich, Germany

<sup>5</sup>Institute of Pathology, Klinikum Bayreuth, Friedrich-Alexander University Erlangen-Nuremberg, Bayreuth, Germany

<sup>6</sup>Klinik für Innere Medizin II, Universitätsklinikum Freiburg, Freiburg, Germany

<sup>7</sup>Chair of Nutrition and Immunology, Technical University of Munich, Freising, Germany

<sup>8</sup>ZIEL Institute for Food & Health, Technical University of Munich, Munich, Germany

<sup>9</sup>Munich Partner Site, German Center for Infection Research (DZIF), Munich, Germany

<sup>10</sup>Institute of Virology, Helmholtz Center Munich - German Research Center for Environmental Health, Neuherberg, Germany

<sup>11</sup>Chair for Preventions of Microbial Diseases, School of Life Sciences, Technical University of Munich, Freising, Germany

**Acknowledgements** We thank members of the laboratory 'Chronic inflammation and carcinogenesis' for experimental help as well as critical discussion, with special thanks to Maximilian Koch, Karin Taxauer, Martin Skerhut and Teresa Burrell for experimental support. We thank Julia Horstmann and the team of the ColoBAC study at the Klinik und Poliklinik für Innere Medizin II, Klinikum rechts der Isar, for the supply of human biopsies. We thank Core Facility Microbiome of the ZIEL Institute for Food & Health, Technical University of Munich, for 16S rRNA sequencing services, as well as Dharmesh Singh and Nyssa Cullin. We thank Core Facility Gnotobiology of the ZIEL Institute for Food & Health, Technical University of Munich, for germ-free mice.

**Contributors** AR, RM-L and MG conceived the study. AR, AD and RM-L designed and analysed experiments. SJ contributed and provided code and support to single cell RNA sequencing and chip cytometry. VE and AW contributed to experiments. SJ and DHB provided methodological expertise. AD, SJ, RM-L and DHB contributed to data interpretation. MV, MM and MQ provided human biopsies. KPJ provided mouse models and critically revised the article. DH, DHB and LD critically revised the article. AR and RM-L wrote the article. AR, RM-L and MG revised the article. MG acquired the funding and is the guarantor of the article. All authors read and reviewed the article.

**Funding** This work was funded by the Deutsche Forschungsgemeinschaft (DFG (German Research Foundation)) SFB 1371/1-395357507 (project P09 and project P04).

**Competing interests** None declared.

**Patient and public involvement** Patients and/or the public were not involved in the design, or conduct, or reporting, or dissemination plans of this research.

**Patient consent for publication** Not applicable.

**Ethics approval** This study was approved by Klinikum rechts der Isar #322/18Klinikum Bayreuth #241\_20Bc. Participants gave informed consent to participate in the study before taking part.

**Provenance and peer review** Not commissioned; externally peer reviewed.

**Data availability statement** Data are available in a public, open access repository. Data are available on reasonable request. Raw single cell RNA sequencing and 16S rRNA sequencing data have been deposited with links to BioProject accession number PRJNA808836 in the NCBI BioProject database (<https://www.ncbi.nlm.nih.gov/bioproject/PRJNA808836/>).

**Supplemental material** This content has been supplied by the author(s). It has not been vetted by BMJ Publishing Group Limited (BMJ) and may not have been peer-reviewed. Any opinions or recommendations discussed are solely those of the author(s) and are not endorsed by BMJ. BMJ disclaims all liability and responsibility arising from any reliance placed on the content. Where the content includes any translated material, BMJ does not warrant the accuracy and reliability of the translations (including but not limited to local regulations, clinical guidelines, terminology, drug names and drug dosages), and is not responsible for any error and/or omissions arising from translation and adaptation or otherwise.

#### ORCID iDs

Klaus Peter Janssen <http://orcid.org/0000-0002-4707-7887>  
 Michael Quante <http://orcid.org/0000-0002-8497-582X>  
 Dirk Haller <http://orcid.org/0000-0002-6977-4085>  
 Raquel Mejias-Luque <http://orcid.org/0000-0002-4602-4927>  
 Markus Gerhard <http://orcid.org/0000-0001-9110-3950>

#### REFERENCES

- Shi Y, Liu X-F, Zhuang Y, et al. Helicobacter pylori-induced Th17 responses modulate Th1 cell responses, benefit bacterial growth, and contribute to pathology in mice. *J Immunol* 2010;184:5121–9.
- Nagai S, Mimuro H, Yamada T, et al. Role of Peyer's patches in the induction of Helicobacter pylori-induced gastritis. *Proc Natl Acad Sci U S A* 2007;104:8971–6.
- Censini S, Lange C, Xiang Z, et al. Cag, a pathogenicity island of Helicobacter pylori, encodes type I-specific and disease-associated virulence factors. *Proc Natl Acad Sci U S A* 1996;93:14648–53.
- Stein M, Rappuoli R, Covacci A. Tyrosine phosphorylation of the Helicobacter pylori CagA antigen after cag-driven host cell translocation. *Proc Natl Acad Sci U S A* 2000;97:1263–8.
- Mejias-Luque R, Zöller J, Anderl F, et al. Lymphotoxin  $\beta$  receptor signalling executes Helicobacter pylori-driven gastric inflammation in a T4SS-dependent manner. *Gut* 2017;66:1369–81.
- Oertli M, Sundquist M, Hitzler I, et al. DC-derived IL-18 drives Treg differentiation, murine Helicobacter pylori-specific immune tolerance, and asthma protection. *J Clin Invest* 2012;122:1082–96.
- Kaebisch R, Mejias-Luque R, Prinz C, et al. Helicobacter pylori cytotoxin-associated gene a impairs human dendritic cell maturation and function through IL-10-mediated activation of STAT3. *J Immunol* 2014;192:316–23.
- Kao JY, Zhang M, Miller MJ, et al. Helicobacter pylori immune escape is mediated by dendritic cell-induced Treg skewing and Th17 suppression in mice. *Gastroenterology* 2010;138:1046–54.
- Oertli M, Noben M, Engler DB, et al. Helicobacter pylori  $\gamma$ -glutamyl transpeptidase and vacuolating cytotoxin promote gastric persistence and immune tolerance. *Proc Natl Acad Sci U S A* 2013;110:3047–52.
- Chen C-C, Liou J-M, Lee Y-C, et al. The interplay between Helicobacter pylori and gastrointestinal microbiota. *Gut Microbes* 2021;13:1–22.
- Lofgren JL, Whary MT, Ge Z, et al. Lack of commensal flora in Helicobacter pylori-infected INS-GAS mice reduces gastritis and delays intraepithelial neoplasia. *Gastroenterology* 2011;140:210–20.
- Gravina AG, Zagari RM, De Musis C, et al. Helicobacter pylori and extragastric diseases: a review. *World J Gastroenterol* 2018;24:3204–21.
- Zuo Y, Jing Z, Bie M, et al. Association between Helicobacter pylori infection and the risk of colorectal cancer: a systematic review and meta-analysis. *Medicine (Baltimore)* 2020;99:e21832.
- Ralsler A, Mejias-Luque R, Gerhard M. Data from: Helicobacter pylori in colorectal carcinogenesis. NCBI BioProject, 2023. Available: <https://www.ncbi.nlm.nih.gov/bioproject/PRJNA808836/>
- Becht E, McInnes L, Healy J, et al. Dimensionality reduction for visualizing single-cell data using UMAP. *Nat Biotechnol* 3, 2018.
- Osman A, Yan B, Li Y, et al. Tcf-1 controls Treg cell functions that regulate inflammation, CD8+ T cell cytotoxicity and severity of colon cancer. *Nat Immunol* 2021;22:1152–62.
- Miragaia RJ, Gomes T, Chomka A, et al. Single-cell transcriptomics of regulatory T cells reveals trajectories of tissue adaptation. *Immunity* 2019;50:493–504.
- Vasanthakumar A, Liao Y, Teh P, et al. The TNF receptor superfamily-NF- $\kappa$ B axis is critical to maintain effector regulatory T cells in lymphoid and non-lymphoid tissues. *Cell Rep* 2017;20:2906–20.
- La Manno G, Soldatov R, Zeisel A, et al. Rna velocity of single cells. *Nature* 2018;560:494–8.
- Parikh K, Antanaviciute A, Fawcner-Corbett D, et al. Colonic epithelial cell diversity in health and inflammatory bowel disease. *Nature* 2019;567:49–55.
- Moor AE, Harnik Y, Ben-Moshe S, et al. Spatial reconstruction of single enterocytes uncovers broad zonation along the intestinal villus axis. *Cell* 2018;175:1156–67.
- Brandt S, Kwok T, Hartig R, et al. NF- $\kappa$ B activation and potentiation of proinflammatory responses by the Helicobacter pylori CagA protein. *Proc Natl Acad Sci U S A* 2005;102:9300–5.
- Menheniott TR, Judd LM, Giraud AS. Stat3: a critical component in the response to Helicobacter pylori infection. *Cell Microbiol* 2015;17:1570–82.
- Bollrath J, Phesse TJ, von Burstin VA, et al. Gp130-Mediated STAT3 activation in enterocytes regulates cell survival and cell-cycle progression during colitis-associated tumorigenesis. *Cancer Cell* 2009;15:91–102.
- Nguyen AV, Wu Y-Y, Liu Q, et al. Stat3 in epithelial cells regulates inflammation and tumor progression to malignant state in colon. *Neoplasia* 2013;15:998–1008.
- Asada R, Saito A, Kawasaki N, et al. The endoplasmic reticulum stress transducer OASIS is involved in the terminal differentiation of goblet cells in the large intestine. *J Biol Chem* 2012;287:8144–53.
- Aden K, Rehman A, Falk-Paulsen M, et al. Epithelial IL-23R signaling licenses protective IL-22 responses in intestinal inflammation. *Cell Rep* 2016;16:2208–18.
- Katoh M, Katoh M. Notch signaling in gastrointestinal tract (review). *Int J Oncol* 2007;30:247–51.
- Wirbel J, Pyl PT, Kartal E, et al. Meta-Analysis of fecal metagenomes reveals global microbial signatures that are specific for colorectal cancer. *Nat Med* 2019;25:679–89.
- Guo Y, Zhang Y, Gerhard M, et al. Effect of Helicobacter pylori on gastrointestinal microbiota: a population-based study in Linqu, a high-risk area of gastric cancer. *Gut* 2020;69:1598–607.
- Ohnmacht C, Park J-H, Cording S, et al. MUCOSAL IMMUNOLOGY. the microbiota regulates type 2 immunity through roryT. *Science* 2015;349:989–93.
- van Zanten SJOV, Kolesnikov T, Leung V, et al. Gastric transitional zones, areas where Helicobacter treatment fails: results of a treatment trial using the Sydney strain mouse model. *Antimicrob Agents Chemother* 2003;47:2249–55.
- Franceschi F, Covino M, Roubaud Baudron C. Review: Helicobacter pylori and extragastric diseases. *Helicobacter* 2019;24 Suppl 1:e12636.
- Kim TJ, Kim ER, Chang DK, et al. Helicobacter pylori infection is an independent risk factor of early and advanced colorectal neoplasm. *Helicobacter* 2017;22.
- Arnold IC, Dehdaz N, Reuter S, et al. Helicobacter pylori infection prevents allergic asthma in mouse models through the induction of regulatory T cells. *J Clin Invest* 2011;121:3088–93.
- Caruso R, Fina D, Paoluzi OA, et al. IL-23-mediated regulation of IL-17 production in Helicobacter pylori-infected gastric mucosa. *Eur J Immunol* 2008;38:470–8.
- Tosolini M, Kirilovsky A, Mlecnik B, et al. Clinical impact of different classes of infiltrating T cytotoxic and helper cells (Th1, Th2, Treg, Th17) in patients with colorectal cancer. *Cancer Res* 2011;71:1263–71.
- Du R, Zhao H, Yan F, et al. IL-17+foxp3+ T cells: an intermediate differentiation stage between Th17 cells and regulatory T cells. *J Leukoc Biol* 2014;96:39–48.
- Ma C, Dong X. Colorectal cancer-derived FOXP3 (+) IL-17 (+) T cells suppress tumour-specific CD8+ T cells. *Scand J Immunol* 2011;74:47–51.

- 40 Yang S, Wang B, Guan C, *et al.* Foxp3+IL-17+ T cells promote development of cancer-initiating cells in colorectal cancer. *J Leukoc Biol* 2011;89:85–91.
- 41 Sinicrope FA, Rego RL, Ansell SM, *et al.* Intraepithelial effector (CD3+)/regulatory (Foxp3+) T-cell ratio predicts a clinical outcome of human colon carcinoma. *Gastroenterology* 2009;137:1270–9.
- 42 Smith G, Carey FA, Beattie J, *et al.* Mutations in APC, Kirsten-ras, and p53 -- alternative genetic pathways to colorectal cancer. *Proc Natl Acad Sci U S A* 2002;99:9433–8.
- 43 Janssen K-P, Alberici P, Fsihi H, *et al.* Apc and oncogenic KRAS are synergistic in enhancing Wnt signaling in intestinal tumor formation and progression. *Gastroenterology* 2006;131:1096–109.
- 44 Schwitalla S, Fingerle AA, Cammareri P, *et al.* Intestinal tumorigenesis initiated by dedifferentiation and acquisition of stem-cell-like properties. *Cell* 2013;152:25–38.
- 45 Eaden JA, Abrams KR, Mayberry JF. The risk of colorectal cancer in ulcerative colitis: a meta-analysis. *Gut* 2001;48:526–35.
- 46 Waldner MJ, Neurath MF. Mechanisms of immune signaling in colitis-associated cancer. *Cell Mol Gastroenterol Hepatol* 2015;1:6–16.
- 47 Kusaba T, Nakayama T, Yamazumi K, *et al.* Activation of STAT3 is a marker of poor prognosis in human colorectal cancer. *Oncol Rep* 2006;15:1445–51.
- 48 Musteanu M, Blaas L, Mair M, *et al.* Stat3 is a negative regulator of intestinal tumor progression in Apc (min) mice. *Gastroenterology* 2010;138:1003–11.
- 49 Chen Y, Vandereyken M, Newton IP, *et al.* Loss of adenomatous polyposis coli function renders intestinal epithelial cells resistant to the cytokine IL-22. *PLoS Biol* 2019;17:e3000540.
- 50 Li Y, Kundu P, Seow SW, *et al.* Gut microbiota accelerate tumor growth via c-Jun and STAT3 phosphorylation in ApcMin/+ mice. *Carcinogenesis* 2012;33:1231–8.
- 51 Compare D, Nardone G. Contribution of gut microbiota to colonic and extracolonic cancer development. *Dig Dis* 2011;29:554–61.
- 52 Wick EC, Rabizadeh S, Albesiano E, *et al.* Stat3 activation in murine colitis induced by enterotoxigenic *Bacteroides fragilis*. *Inflamm Bowel Dis* 2014;20:821–34.
- 53 Iino C, Shimoyama T. Impact of *Helicobacter pylori* infection on gut microbiota. *World J Gastroenterol* 2021;27:6224–30.
- 54 Kienesberger S, Cox LM, Livanos A, *et al.* Gastric helicobacter pylori infection affects local and distant microbial populations and host responses. *Cell Rep* 2016;14:1395–407.
- 55 Uronis JM, Mühlbauer M, Herfarth HH, *et al.* Modulation of the intestinal microbiota alters colitis-associated colorectal cancer susceptibility. *PLoS One* 2009;4:e6026.
- 56 Wang L, Tang L, Feng Y, *et al.* A purified membrane protein from *Akkermansia muciniphila* or the pasteurised bacterium blunts colitis associated tumourigenesis by modulation of CD8+ T cells in mice. *Gut* 2020;69:1988–97.
- 57 Weir TL, Manter DK, Sheflin AM, *et al.* Stool microbiome and metabolome differences between colorectal cancer patients and healthy adults. *PLoS One* 2013;8:e70803.